Dynamic Behavior and Locking of a Semiconductor Laser Subjected to External Injection

Valerio Annovazzi-Lodi, *Member, IEEE*, Alessandro Sciré, Marc Sorel, and Silvano Donati, *Member, IEEE*

***Abstract*— In this paper, we analyze the phenomena arising when a monomode semiconductor laser is subjected to external injection from another laser. The system stability is investigated as a function of detuning and of the relative injected power. Different regimes, spanning from phase locking to chaos and coherence collapse, are described by analytical and numerical methods for weak and moderate injection. Previous theoretical studies are extended by describing the inverse transition from chaos to stability and by deriving the final locking condition. Also, further investigation on the coherence collapse regime has been performed. Besides contributing to the exploration of an interesting fundamental phenomenon, the results of this analysis are useful for different applications, including coherent detection and chaotic cryptography.**

***Index Terms*— Chaos, injection locking, laser stability, semiconductor laser.**

I. Introduction

INJECTION semiconductor laser (ISL) systems have been widely investigated [1]–[11] since the early 1980's because of their role in coherent detection, and in view of promising applications such as laser spectral narrowing, modulation bandwidth widening, reduction of partition noise, and of frequency chirping.

Early theoretical analysis showed that a stable phase locking between master and slave sources [Fig. 1(a)] cannot be achieved for all parameter values because of instabilities caused by the laser nonlinearities.

Injection phenomena in lasers are governed by the competition between the amplification of the spontaneous emission, the injected signal, and their beating. Moreover, specific phenomena must be taken into account, such as the gain-change effect in the semiconductor laser. The resulting dynamic behavior has been investigated theoretically, finding a route from stability to coherence collapse at increasing injection levels. Different regimes have been described, including self-pulsations and chaos. Recently, the chaotic behavior of such a system has also been proposed for cryptographic applications [8]. However, little information is available in the literature for higher injection levels. Though a reverse route from instability to a final locking has been found numerically [5], the upper boundaries of the instability region have not yet been found analytically.

In the following, we describe the dynamic behavior of a semiconductor laser subjected to external injection as a function of detuning $\Delta\omega$ and of the relative amplitude of the injected field K. Results are summarized as usual by the locking diagram $(K, \Delta\omega)$ of the forced oscillator, where we will find different zones, as shown in Fig. 1 (weak injection) and Fig. 2 (weak to moderate injection), namely:

1) *stable locking zones*, where the slave laser locks in phase to the master and the dynamic variables describing the system reach a constant value;
2) *a beating zone*, where the slave laser is amplitude modulated at the detuning frequency [5];
3) *self pulsation zones*, where the field of the slave laser oscillates at the relaxation frequency;
4) *chaotic zones*, where the oscillation becomes chaotic after a route which includes period doubling and multiperiodical regime [3], [5];
5) *a coherence collapse zone*, where the slave phase shows strong fluctuations and its spectrum becomes wide.

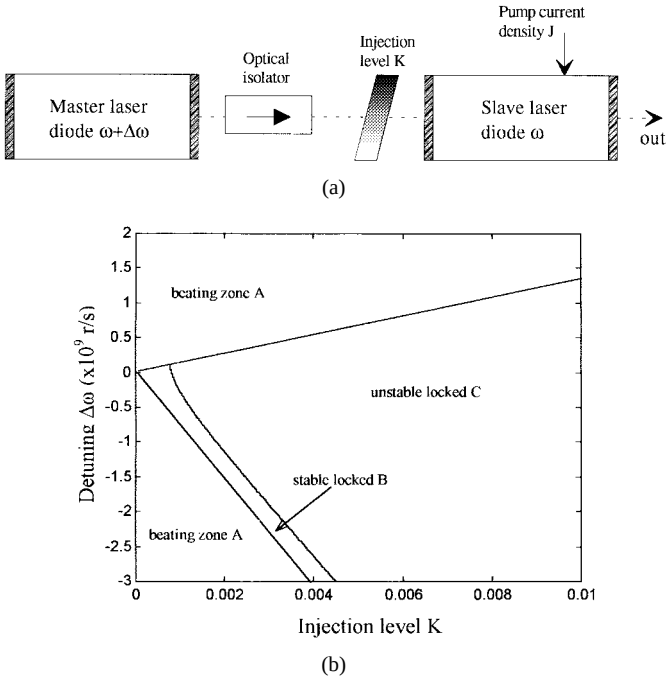

Fig. 1. (a) Injection setup. (b) Locking diagram for weak injection, showing three different regimes: A: beating zone at the detuning frequency; B: first stable locking range; C: unstable locked zone.

II. Injection in Semiconductor Lasers

A suitable model for a semiconductor laser subjected to light injection by reflection from an external mirror has been proposed by Lang and Kobayashi [9], and it can be easily

Manuscript received April 24, 1998; revised July 28, 1998. This work was supported by MURST under an ex-40% contract.

The authors are with the Dipartimento di Elettronica, Universitá di Pavia, Pavia, Italy.

Publisher Item Identifier S 0018-9197(98)08674-6.

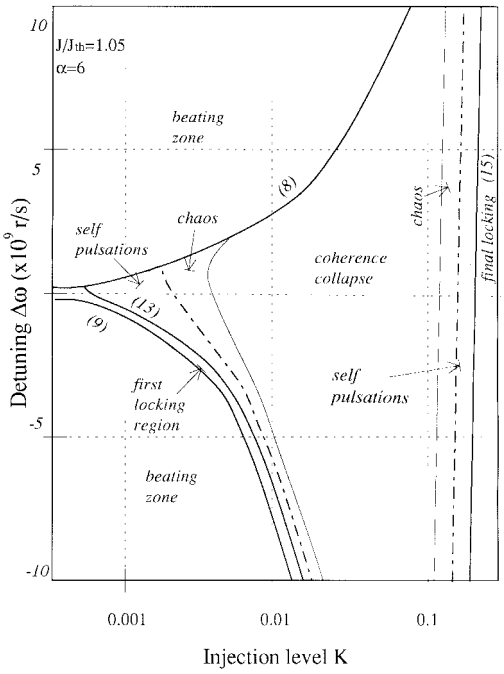

Fig. 2. Complete locking diagram showing the dynamics for weakly to moderate injection. The unstable locked zone includes the dynamics of a typical nonlinear oscillator : self-pulsations (i.e., a torus in the phase space), chaotic oscillations, and coherence collapse. The final stable locking zone is reached for a moderate injection level. Numbers into parentheses indicate the corresponding equation of the text.

modified to describe the ISL of Fig. 1(a) [3], [5], [12], obtaining the following set of equations:

$$\frac{dE_{\text{laser}}}{dt} = \frac{1}{2}[G_n(N_{\text{laser}} - N_0) - 1/\tau_p]E_{\text{laser}} + \frac{K}{\tau_{\text{in}}}E_{\text{inj}}\cos(\phi)$$

$$\frac{d\phi}{dt} = \frac{1}{2}\alpha[G_n(N_{\text{laser}} - N_0) - 1/\tau_p] - \frac{K}{\tau_{\text{in}}}\frac{E_{\text{inj}}}{E_{\text{laser}}}\sin(\phi) - \Delta\omega$$

$$\frac{dN_{\text{laser}}}{dt} = R_p - \frac{N_{\text{laser}}}{\tau_S} - G_n(N_{\text{laser}} - N_0)E_{\text{laser}}^2$$

where E_{laser} and ϕ are the laser electric field amplitude and phase, N_{laser} is the population inversion, E_{inj} is the amplitude of the external injecting field, while definitions of other parameters are reported in Table I. As shown in Fig. 1(a), K represents the transmission of the master laser output (including all attenuation sources), and its value determines the injected field KE_{inj} into the slave. Transmission K has been found to be a suitable order parameter of the chaos transition for the ISL system [3], [5].

In carrying out the analytical calculations, we have found it convenient to normalize the dynamic variables as follows:

$$e = (E_{\text{laser}} - E_{\text{sol}})/E_{\text{sol}}$$
$$n = (N_{\text{laser}} - N_{\text{th}})/N_{\text{th}}$$

where E_{sol} and N_{th} are the solitary laser static values for the electric field and for the carrier density, i.e., the solutions of the first and third equations of the Lang–Kobayashi model without injection. To simplify calculations, E_{inj} has been taken equal to that of the solitary laser E_{sol}, without lack of generality. After some algebra, we obtain a new set which will be used throughout our paper to describe the ISL, i.e.,

$$\frac{de}{dt} = Gn(e+1) + k\cos\phi \quad (1)$$

$$\frac{d\phi}{dt} = \alpha Gn - \frac{k}{e+1}\sin\phi - \Delta\omega \quad (2)$$

$$\frac{dn}{dt} = -\frac{n}{T^*} - \omega_R^2(\tau_P n + 1/2G)e(e+2) \quad (3)$$

where

$$\omega_R^2 = G_n E_{\text{sol}}^2/\tau_P$$
$$1/T^* = 1/\tau_S + \omega_R^2\tau_P.$$

In these equations, parameter ω_R is the relaxation oscillation frequency of the slave laser, T^* is its relaxation time, G_n is the differential gain, obtained from linearization of the carrier density gain dependence, while the frequency dependence of the gain has been neglected as usual [10]; $\Delta\omega$ is the nominal uncoupled detuning between the two lasers.

For clarity, definitions of the main parameters and variables used throughout this paper have been summarized in Table I, where typical values, which have been used in simulations and as a guideline to make approximations in the theoretical

TABLE I
LASER PARAMETERS

$G = 13.91 \times 10^{11}$ [s^{-1}]	normalized differential gain, $G = 0.5G_n N_{\text{th}}$
$N_{\text{th}} = 1.7172 \times 10^{24}$ [m^{-3}]	threshold carrier density, $N_{\text{th}} = 1/G_n\tau_P + N_0$
$G_n = 8.1 \times 10^{-13}$ [m^3/s]	differential gain
$\tau_P = 2$ ps	photon lifetime
$N_0 = 1.1 \times 10^{24}$ [m^{-3}]	carrier density at transparency
$E_{\text{sol}} = [(R_P - N_{\text{th}}/\tau_s)\tau_P]^{1/2}$ [m$^{-3/2}$]	unperturbed electric field amplitude
$\tau_s = 2$ ns	electron–hole recombination time
$R_P = J\eta/qd$ [(m^3 s)$^{-1}$]	pump parameter (J = pump current density, q = electron charge, d = active region thickness, η = efficiency)
$R_{P\text{th}} = J_{\text{th}}\eta/qd$ [(m^3 s)$^{-1}$]	laser pump parameter at threshold
J_{th} [A/m^2]	laser current density at threshold
$\tau_{\text{in}} = 8$ ps	round-trip time in the laser cavity
$K =$ from 0 to 0.2	field transmission factor of injected light
$k = K/\tau_{\text{th}}$ [m^3/s]	external injection rate
$\Delta\omega$ [r/s]	nominal detuning
$\alpha = 6$	linewidth enhancement factor
T^* [s]	relaxation time
ω_R [r/s]	laser relaxation frequency
ω_{R0} [r/s]	actual resonance frequency of eq. (18)
ω_C [r/s]	instantaneous frequency of phase fluctuation in the coherence collapse regime
$J_0 = J/J_{\text{th}}$	normalized density current
K_0	injection level at the final locking
$e,\ \phi,\ n$	normalized electric field amplitude, phase and carrier density of the laser subjected to external injection
$e_s,\ \phi_s,\ n_s$	stationary points of the laser dynamic variables

analysis, are also reported. In our simulations, the gain-suppression term $\varepsilon\Gamma \approx 10^{-24}$ has been neglected since it gives only a very small correction to (1)–(3).

The Lang–Kobayashi equations represent a simple and generally accepted model in the literature to describe a semiconductor laser. Since the aim of this paper is to gain physical insight by analytical calculations and fast numerical analysis, we have not tried to develop a more accurate model including noise sources or describing the laser technology. We remark that our model is monomodal and quasi-monocromatic, so it cannot describe phenomena such as four-wave mixing or wavelength bistability, which have been experimentally observed. In addition, throughout our analysis we will neglect, as usual, spontaneous emission [10] as well as radiative and nonlinear Auger recombination. In spite of these limitations, it will be shown that the model includes all relevant phenomena, either observed experimentally or predicted theoretically in the weak to moderate injection regimes [3]–[7], including chaos, coherence collapse, bistability, and the final locking. Moreover, the general behavior of the ISL is not critically dependent on the values of parameters. Nevertheless, model refinements would be necessary to get quantitative matching with experimental measurements on specific sources (such as Fabry–Perot or distributed feedback (DFB) lasers), especially in the region of large injection $(K > 0.1)$ and detuning $(\Delta\omega > 5$ GHz).

A slave laser can be forced by injection to oscillate at a master laser frequency by two different phenomena. The first is typical of most oscillators and has been first described by Adler [13] for RF circuits. Injecting a fraction K of the master output electric field into the slave adds to the oscillating field an out-of-phase contribution for unit time (normalized to the unperturbed master output) $k = K/\tau_{\text{in}}$, where τ_{in} is the cavity round trip. Such a perturbation can result in phase locking of the slave to the master [13].

The other phenomenon (gain-change effect [14]) is specific to semiconductor lasers and is due to the dependence of the refractive index of the active medium on carrier density [15]; namely, the injected power partially depletes the population inversion, varying the complex refractive index, which results in a negative shift of the cavity frequency, which affects on its turn both detuning and the locking condition. This effect is described by the linewidth enhancement factor α [14]. In semiconductor lasers, the second effect is dominant for $\alpha > 1$, giving rise to a peculiar asymmetric locking diagram and to dynamic instabilities [9], [10].

III. Stationary Points

We start our analysis by finding the stationary solutions of the system, which will be denoted in the following by e_s, n_s, and ϕ_s. Setting to zero the derivatives of the dynamic variables in (1)–(3), we find from (1) and (2) a relation between e and n. Solving for n and substituting into (3), we get a sixth-order polynomial in the variable e, which admits six solutions. However, since the problem is mathematically folded with respect to $e = -1$ (i.e., $E_{\text{laser}} = 0$), we only need to consider the three solutions for $e > -1$.

Of these roots, one is nearly unitary $(e_s \approx -1)$ and must be dropped since its associated gain shift (the stationary value of n_s which corresponds to that value of e_s) is negative [2], and the others are symmetrical with respect to $e = 0$ (i.e., $E_{\text{laser}} = E_{\text{sol}}$). These roots can be determined by approximating the polynomial in e to the second order, obtaining

$$e_s = \frac{\alpha\Delta\omega}{T^*(1+\alpha^2)\omega_R^2}\left(-1 \pm \sqrt{1 + \frac{(k^2 - \Delta\omega^2)(1+\alpha^2)}{\alpha^2\Delta\omega^2}}\right). \tag{4}$$

Since, even in a considerably wide injection versus detuning window, $e_s \ll 1$, substituting into (3) gives

$$n_s = -\frac{T^*\omega_R^2 e_s}{G} \tag{5}$$

while from (2) we obtain the well-known stationary Adler's equation [7]

$$\Delta\omega = \frac{k}{e_s + 1}(\alpha\cos\phi_s - \sin\phi_s) \tag{6}$$

which gives ϕ_s in implicit form.

IV. Stability Analysis for Weak Injection

We are now going to evaluate the locked stationary solutions, i.e., the *real* solutions of (4)–(6). For $K < 10^{-2}$ (weak injection), the laser amplitude perturbation is very small and (6) becomes

$$\Delta\omega = k\sqrt{1+\alpha^2}\sin(\phi_s - a\tan\alpha). \tag{7}$$

The region where (7) admits real solutions is bounded in the $(k,\ \Delta\omega)$ plane by the two half-lines [2]

$$\Delta\omega = k, \quad \text{for } \Delta\omega > 0 \tag{8}$$

$$\Delta\omega = -k\sqrt{1+\alpha^2}, \quad \text{for } \Delta\omega < 0. \tag{9}$$

Outside this region we find the well-known beating zone [5] (marked A in Fig. 1), where the injection level is too low, or detuning is too high, to get locking. Inside this region, the system allows at least one real solution set $(e_s,\ n_s,\ \phi_s)$, i.e., a stationary point, and in the following we will evaluate its stability.

The classical eigenvalue analysis can be developed to this purpose. We consider the Jacobian matrix associated with the nonlinear set (1)–(3), shown as (10), at the bottom of the page, which must be evaluated in the stationary point ($e = e_s$, $\phi = \phi_s$, and $n = n_s$) with k and $\Delta\omega$ as parameters.

$$J = \begin{bmatrix} Gn & k\sin\phi & G(e+1) \\ -\frac{k}{(e+1)^2}\sin\phi & -\frac{k}{e+1}\cos\phi & \alpha G \\ -2\omega_R^2(\tau_P n - 1/2G)(e+1) & 0 & -1/T^* - \omega_R^2\tau_P e(e+2) \end{bmatrix} \tag{10}$$

If $(k,\ \Delta\omega) = (0,0)$, we have a solitary laser which is asymptotically stable, as expected, since one eigenvalue is zero while the others lie in the left half of the complex plane. As k and $\Delta\omega$ are varied, the eigenvalues become complex conjugates and can possibly reach the right half plane and give rise to instabilities; however, we expect a final locking for sufficiently strong injection, as supported by experimental evidences and numerical analysis [5].

The eigenvalues can be obtained as the roots of the secular determinant of J [16]

$$D(s) = s^3 + As^2 + Bs + C \tag{11}$$

where $A = \mathrm{tr}(J)$, $B = \sum_i m_{ii}$ is the sum of the minors of the matrix diagonal m_{ii}, and $C = \det(J)$. From (10), the expressions of these parameters can be found as

$$A = \omega_R^2 + k^2(e_s+1)^2 + \frac{2k(e_s+1)}{T^*}\cos\phi_s$$
$$B = \frac{1}{T^*} + 2k(e_s+1)\cos\phi_s$$
$$C = \left[\frac{k(e_s+1)^2}{T^*}\right] + (1 + 2G\tau_P n_s)k\omega_R^2(\cos\phi_s - \alpha\sin\phi_s).$$

To find the stability boundary of the system, we determine the imaginary-axis crossing condition of the roots of (11), i.e.,

$$A_{k,\Delta\omega}B_{k,\Delta\omega} = C_{k,\Delta\omega}. \tag{12}$$

Equation (12) represents a locus in the $(k,\ \Delta\omega)$ which, under the assuption $K < 10^{-2}$ (weak injection), can be approximated by the following hyperbole:

$$k^2 - \left(\frac{\Delta\omega}{(1-\alpha^2)} - \frac{2\alpha}{T^*(1-\alpha^4)}\right)^2 = \frac{1}{T^{*2}(1+\alpha^2)}. \tag{13}$$

The $(k,\ \Delta\omega)$ plane region bounded by (13) and (8) is generically unstable (zone C in Fig. 1) while zone B in Fig. 1 is the first stable locking region [2].

Due to our assumption of weak injection, we cannot find the boundary of zone C for higher K. In the following, we will extend this theory to describe the dynamical behavior in the moderate injection regime, to get more insight into the ISL stability.

V. Stability Analysis for Moderate Injection

To carry on the analysis for $K > 10^{-2}$, we use the expressions of the stationary values of n_s, ϕ_s given by (5) and (6), while (4) can be symplified as follows:

$$e_s(m.i.) \approx \frac{k}{T^*\sqrt{1+\alpha^2\omega_R^2}}, \qquad \text{for } k = \frac{K}{\tau_{\mathrm{in}}} \gg \Delta\omega \tag{14}$$

a condition which for moderate injection is satisfied even for a considerably large detuning, such as $\Delta\omega = 10$ GHz.

In the moderate injection approximation, ω_R^2 can be neglected in A and $1/T^*$ can be neglected in B. Substituting n_s, ϕ_s, and e_s, we can write A, B, and C as functions of k, $\Delta\omega$.

Then, from (12), we get once again a curve in the plane $(k,\ \Delta\omega)$, which represents the stability limit for our system. The analytical expression of such a curve appears to be the ratio of a third-order polynomial in k divided by a factor $1+Pk$ (where P is a constant and $Pk \ll 1$); thus, it represents a clockwise-rotated cubic curve. Even if we consider a wide injection versus detuning window, such as ($K = 0 \Rightarrow 0.3$, $\Delta\omega = -10 \Rightarrow 10$ GHz), it is found that only the positive branch of this locus is of interest. Moreover, this curve can be linearized with small error (less than 0.3%, with our parameter set), by a first-order Taylor approximation around its intersection with the axis $\Delta\omega = 0$, obtaining

$$\Delta\omega = m(k - k_0) \tag{15}$$

where

$$k_0 = \frac{5\sqrt{1+\alpha^2}}{4T^*}\left(1 + \frac{2\sqrt{2}}{5}T^*\omega_R\right) \tag{16}$$

$$m = \frac{\sqrt{1+\alpha^2}}{\alpha}\left(-\frac{25}{8(T^*\omega_R)^2} + \frac{5\sqrt{2}}{2T^*\omega_R} + 2\right). \tag{17}$$

The final locking region is thus on the right side of the straight line described by (15), as shown in Fig. 2. The angular coefficient of this line is positive; this is consistent with the well-known observation that it is easier to lock an ISL by a negative detuning because of the negative shift of the optical frequency caused by the injection itself [10], [11]. The zone bounded by the hyperbole (13) and by the line (15) does not allow negative real part eigenvalues, and thus the stability analysis developed so far cannot predict in detail the dynamic behavior of the system. In the following, we will analyze this region by a different approach, with a special emphasis on the large coherence collapse zone it includes.

VI. Instability and Chaotic Phenomena

The ISL model is a dynamic, dissipative, nonlinear system defined in a three-dimensional (3-D) space. For increasing K, a scenario typical of many 3-D nonlinear oscillators [17], [18] has been found numerically, confirming previously reported results [3]–[7]. Moreover, we have also accurately verified, directly from set (1)–(3), the approximated analytical results of the previous sections. The ISL behavior is shown in Fig. 2.

On the left side of the hyperbole (13), the system is asymptotically stable, represented by a focus point in phase space. Just after the hyperbole, an oscillatory behavior, close to the relaxation frequency of the system, is found, which leads to a limit cycle [Fig. 3(a)]. For increasing K, the limit cycle widens into a single toroidal surface and, by further increasing K, period doubling [Fig. 3(b)] and multiple toroidal surfaces [Fig. 3(c)] are found. This zone is labeled "self-pulsations" in Fig. 2. Finally, when the so-called "torus break-down" [19] is reached (the first dashed–dotted line in Fig. 2), the system enters the chaotic regime [Fig. 3(d)]. It has been verified that the necessary conditions set by the Shilnikov theorem [17], [18] are satisfied by the ISL in all the zones marked "chaos" in Fig. 2.

All the complex behaviors described in this section are the prelude to another interesting phenomenon called the "coherence collapse," often classified as chaos, but actually

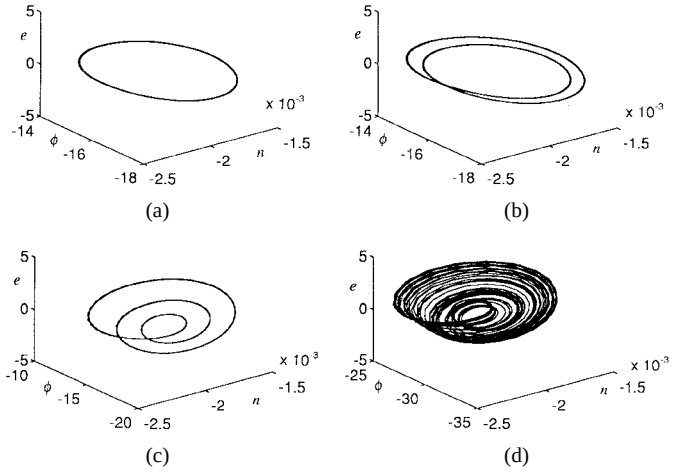

Fig. 3. System behavior as a function of K in the phase space: (a) limit cycle, (b) single torus, (c) multitorus regime, and (d) chaos.

very different from both the mathematical and the physical point of view. This regime will be analyzed in Section VII.

After this region, for still larger values of K, the system follows an inverse route to more stable regimes [5], passing through a second chaotic region, a second self-pulsation region, and finally reaching the definitive locking (15).

VII. Coherence Collapse

The largest zone of the locking diagram of Fig. 2 is occupied by a regime called coherence collapse. The fluctuations of the dynamic variables found in the neighboring chaotic zones are widely exceeded in this region, where the phase of the slave laser is subjected to large temporal variations, resulting in a very wide and irregular spectrum. This is shown in Fig. 4(a) and (b) where we report simulations in the phase space and the time domain, which should be compared with the chaotic attractor of Fig. 3(d).

To study this regime, (1) and (3) have been converted into a single second-order differential equation, i.e.,

$$\left(\frac{d^2}{dt^2}+\frac{1}{T^*}\frac{d}{dt}+\omega_R^2\right)n(t)=-\frac{k}{\tau_P}\cos\phi(t). \tag{18}$$

The first term of (18) represents a damped oscillator, with a free oscillation close to ω_R and a damping factor $1/T^*$. The second term is a periodic forcing term in $\phi(t)$, with instantaneous frequency $d\phi/dt$, as given by (2), which, for $e_s \ll 1$, becomes

$$\frac{d}{dt}\phi=-\Delta\omega+\alpha G n(t)-k\sin\phi(t). \tag{19}$$

An analytical solution of (18) has been found [6] for a generic function of time $\phi(t)$, i.e.,

$$n(t)=-\frac{k\omega_R^2}{G\omega_{\mathrm{RO}}}e^{\frac{-t}{T^*}}\cos(\omega_{\mathrm{RO}}t)\otimes\cos(\phi(t)) \tag{20}$$

where $\otimes$ is the convolution operator and ω_{RO} is the actual resonant frequency of the first member of (18)

$$\omega_{\mathrm{RO}}=\sqrt{\omega_R^2+\left(\frac{1}{2T^*}\right)^2}=\omega_R. \tag{21}$$

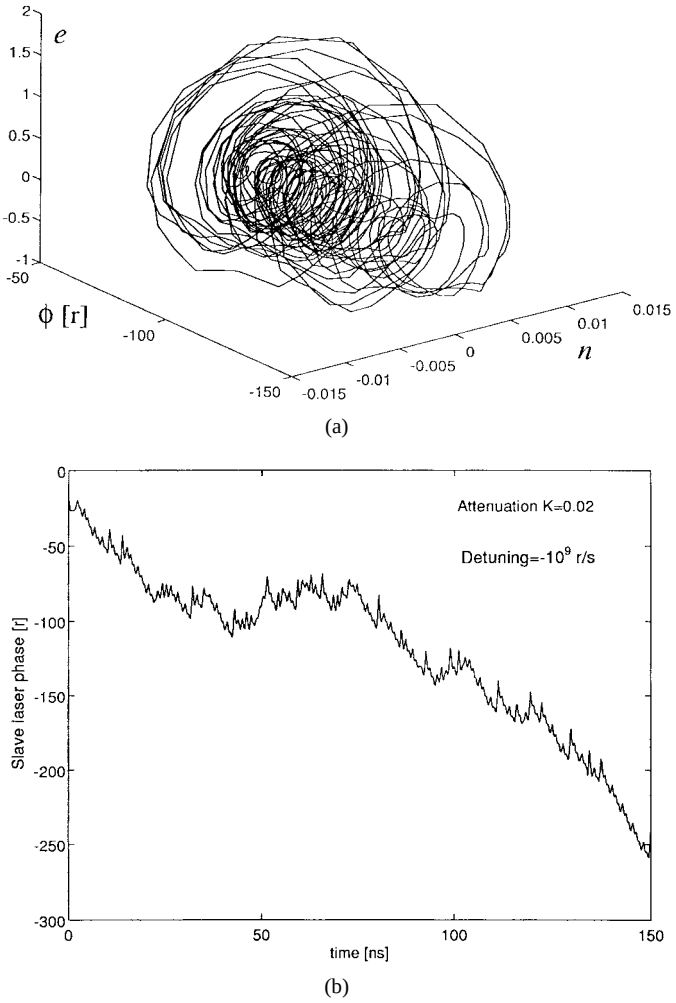

Fig. 4. Coherence collapse regime: (a) phase plane diagram and (b) time-domain diagram.

By writing the phase as $\phi(t)=\omega_C t+\phi_O$, where ω_C is a generic function of time and ϕ_O is a constant, developing the convolution in (20), and inserting the expression of n into (19), a more convenient form is obtained for (19), i.e.,

$$\frac{d}{dt}\phi=-\Delta\omega+k(\alpha R(t)-\sin\phi(t)) \tag{22}$$

where $R(t)=Gn(t)/k$ is given by

$$R(t)=\frac{\left(\left(\frac{\omega_c}{\omega_R}\right)^2-1\right)\cos\phi(t)-\frac{\omega_c}{\omega_R T^*}\sin\phi(t)}{\left(\left(\frac{\omega_c}{\omega_R}\right)^2-1\right)^2+\left(\frac{\omega_c}{\omega_R T^*}\right)^2}. \tag{23}$$

It is interesting to note that for $\omega_C=0$ it is $R(t)=\cos\phi$ and $d\phi/dt=0$, so that (22) reverts to the Adler stationary equation of Section III.

By straightforward calculations, (22) can be alternatively written in the form

$$d\phi/dt=-\Delta\omega+k\rho_\omega\sin(\phi+\gamma_\omega). \tag{24}$$

Equation (24) is a dynamic Adler equation, which describes the phase relationship between the master and the slave laser

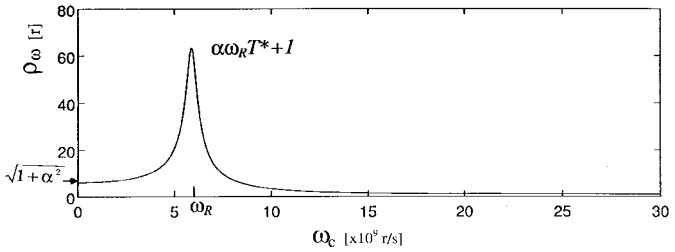

(a)

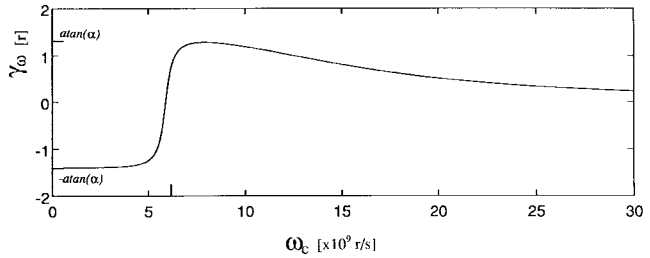

(b)

Fig. 5. Parameters ρ_ω and γ_ω of the dynamic Adler equation as a function of frequency ω_c. For ρ_ω, $\alpha\omega_r T^* + 1$ is the peak value, while $(1+\alpha^2)^{1/2}$ is the low frequency value $(\omega_c \to 0)$.

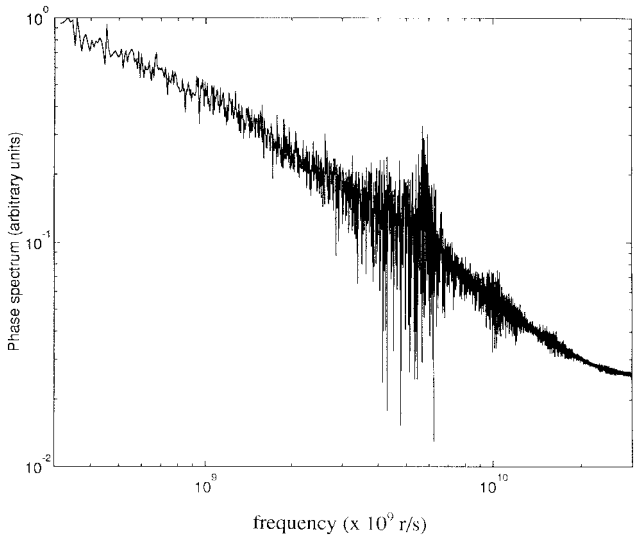

Fig. 6. Phase spectrum in the coherence collapse regime.

and includes the gain-change effect and the resonance between the electric field and carriers. The expressions of ρ_ω and γ_ω are reported in the appendix for completeness.

Parameters ρ_ω and γ_ω represent amplitude and phase modulation terms in (24). They have been plotted in Fig. 5 as functions of ω_c to show their typical resonance behavior. For $d\phi/dt = 0$, the locking condition is met and $\phi = 0$, $\gamma_0 = a\tan(\alpha)$, and $\rho_0 = (1+\alpha^2)^{1/2}$, in accordance to (7).

The complete study of (24) is rather difficult, since it is not correct to assume a solution at a constant or slowly varying frequency $\omega_c = \omega_R$ and impose the sine function between ± 1, in order to find the limits of existence. Indeed, if we assume that (24) admits a regime solution with instantaneous frequency close to ω_R, the very fast phase jumps due to the steep slope of γ_ω around ω_R, drastically increasing the spectral content of ϕ. As a consequence, the instantaneous frequency of ϕ varies rapidly and is actually very different from ω_R, which invalidates our assumption.

As a matter of fact, the coherence collapse regime consists of complicated oscillations which spread over a wide frequency range; this can be appreciated from phase–plane and time-domain plots (Fig. 4) and is especially evident from the phase spectrum, which has been obtained by fast Fourier transformation (FFT) after numerical integration of (24), and is shown in Fig. 6.

From another point of view, the coherence collapse can be viewed as a regenerative phenomenon taking place in the slave laser, which is triggered by the external perturbation due to the master laser. Indeed, (24) describes a system with feedback, where a variation of ϕ determines a change in $d\phi/dt$ which on its turn gives a new variation of ϕ. From (24), it is found that the condition to sustain oscillations is

$$I = K\alpha\omega_R T^* > 1 \tag{25}$$

for small detuning and moderate injection.

From (25), we conclude that coherence collapse is triggered if transmission K is large enough, and the dumping factor of the system $1/T^*$ is small enough to get a gain loop $I > 1$. If (25) is not satisfied, the coherence collapse regime cannot take place. Note that, though (24) was written assuming that the system was inside the region confined between the straight lines (8) and (9), in (25) there is no direct dependence on detuning $\Delta\omega$.

It is worth noting that information about the upper frontier of the coherence collapse cannot be derived from (24), because this equation does not contain information about the trajectories of the eigenvalues. The straight line (15) in the $(k, \Delta\omega)$ plane was in fact obtained in Section V following a different approach.

VIII. Final Remarks and Conclusions

This paper represents a new and more extended analysis of the dynamics of a semiconductor laser subjected to external injection. We have derived analytical results for the return route to stability for moderate injection and have presented complete locking diagrams showing all the different regimes of the injection system.

The locking diagrams reported in Fig. 2 have been drawn in a window in the $(k,\ \Delta\omega)$ plane, where separate first and final stable locking regions have been found. To investigate the system behavior outside this region, we have integrated numerically the set (1)–(3). We have found that the two locking regions actually join for strong negative detuning (Fig. 7). The locking diagram is very sensitive to α and to the normalized pump $J_0 = J/J_{\rm th}$. For increasing α, the stable locked zones get thinner, while for increasing J_0 the final stable locked zone is reached for higher K values. We have determined the analytical dependence of K_0, i.e., the injection level for which the final locking is reached [see (15)], from α and J_0, finding

$$K_0 = 0.8\tau_{\rm in}\sqrt{(1+\alpha^2)G_n R_{p\,\rm th}}\sqrt{J_0 - 1}, \quad \Delta\omega = 0.$$

Finally, we show in Fig. 8 how the locking diagram changes by varying parameters α and J_0. Though for $K > 0.2$ the

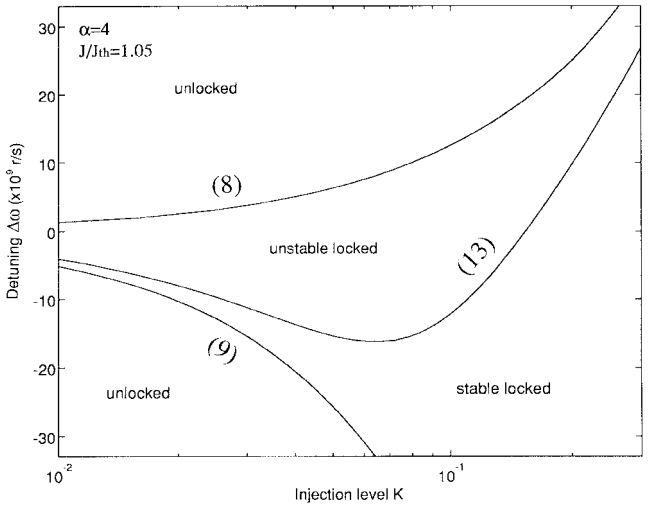

Fig. 7. Locking diagram in an extended window. Curves are labeled to allow a comparison with Fig. 2.

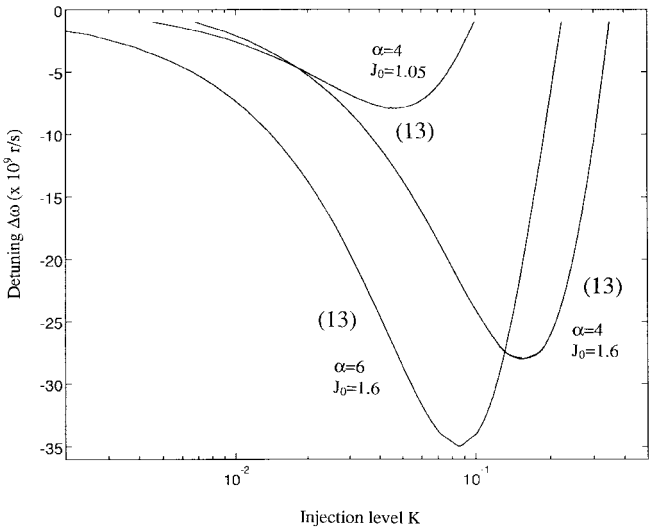

Fig. 8. Locking diagram as a function of α and J_0. Curves are labeled to allow a comparison with Figs. 2 and 7.

model accuracy is questionable, it is interesting to note that the shape of the diagram is not strongly modified and that a final locking is always predicted.

APPENDIX

Letting $X = [(\omega_c/\omega_r)^2 - 1]$, $Y = \omega_c/(\omega_r T^*)$, and by using (23), (22) can be written in the form (24) with

$$\rho_\omega = \sqrt{\left(\frac{\alpha X}{X^2+Y^2}\right)^2 + \left(\frac{\alpha Y}{X^2+Y^2} - 1\right)^2}$$

$$\gamma_\omega = a\tan\left(\frac{\alpha Y - X^2 - Y^2}{\alpha X}\right).$$

REFERENCES

[1] G. H. M. Tartwijk and D. Lensto, "Semiconductor laser with optical injection and feedback," *Quantum Semiclass. Opt.*, vol. 7, pp. 87–143, July 1995.

[2] F. Mogensen, H. Olesen, and G. Jacobsen, "Locking conditions and stability properties for a semiconductor laser with external light injection," *IEEE J. Quantum Electron.*, vol. QE-21, pp. 748–793, July 1985.

[3] J. Sacher, D. Baums, P. Panknin, W. Erlasser, and E. O. Gobel, "Intensity instabilities of semiconductor lasers under current modulation, external light injection, and delayed feedback," *Phys. Rev. A*, vol. 45, no. 3, pp. 1893–1905, Feb. 1992.

[4] K. Peterman, "External optical feedback phenomena in semiconductor lasers," *IEEE J. Select. Topics Quantum Electron.*, vol. 1, pp. 480–489, June 1995.

[5] V. Annovazzi-Lodi, S. Donati, and M. Manna, "Chaos and locking in a semiconductor laser due to external injection," *IEEE J. Quantum Electron.*, vol. 30, pp. 1537–1541, July 1994.

[6] B. Tromborg and J. Mørk, "Nonlinear injection locking dinamics and the onset of coherence collapse in external cavity lasers," *IEEE J. Quantum Electron.*, vol. 26, pp. 642–654, Apr. 1990.

[7] L. Li, "A unified description of a semiconductor laser with external light injection and its application to optical bistability," *IEEE J. Quantum Electron.*, vol. 30, pp. 1723–1731, Aug. 1994.

[8] V. Annovazzi-Lodi, S. Donati, and A. Sciré, "Synchronization of chaotic injected laser systems and its application to optical cryptography," *IEEE J. Quantum Electron.*, vol. 32, pp. 953–959, June 1996.

[9] R. Lang and K. Kobayashi, "External optical feedback effects on semiconductor injection laser properties," *IEEE J. Quantum Electron.*, vol. QE-16, pp. 347–355, Mar. 1980.

[10] R. Lang, "Injection locking properties of a semiconductor laser," *IEEE J. Quantum Electron.*, vol. QE-18, pp. 976–983, June 1983.

[11] C. H. Henry, N. A. Olsson, and N. K. Dutta, "Locking range and stability of injection locked 1.54 μm InGaAsP semiconductor laser," *IEEE J. Quantum Electron.*, vol. QE-21, pp. 1152–1156, Aug. 1985.

[12] M. B. Spencer and W. E. Lamb, "Laser with a transmitting window," *Phys. Rev.*, vol. 5, no. (II), pp. 884–893, Feb. 1972.

[13] R. Adler, "A study of locking phenomena in oscilllators," in *Proc. IRE*, June 1946, vol. 34, pp. 351–356.

[14] K. Vahala, L. C. Chiu, S. Margalit, and A. Yariv, "On the linewidth enhancement factor in semiconductor injection lasers," *Appl. Phys. Lett.*, vol. 42, pp. 631–633, Apr. 1983.

[15] C. H. Henry, R. A. Loga, and K. A. Bertenss, "Spectral dependence of the change in refractive index due to carrier injection in GaAs lasers," *J. Appl. Phys.*, vol. 52, pp. 4457–4460, July 1981.

[16] G. A. Korn and T. M. Korn, *Mathematical Handbook for Scientists and Engineers*. New York: McGraw-Hill, 1968.

[17] S. Wiggins, *Introduction to Non Linear System Dynamics and Chaos*. Berlin, Germany: Springer-Verlag, 1991.

[18] C. P. Silva, "Shilnikov theorem—A tutorial," *IEEE Trans. Circuits Syst. I*, vol. 40, pp. 675–682, Oct. 1993.

[19] V. S. Anishchenko, M. A. Safonova, and L. O. Chua, "Confirmation of the Afraimovich-Shilnikov Torus-Breakdown Theorem via a Torus Circuit," *IEEE Trans. Circuits Syst. I*, vol. 40, pp. 792–800, Nov. 1993.

Valerio Annovazzi-Lodi (M'89) was born in Novara, Italy, on November 7, 1955. He received the degree in electronic engineering from the University of Pavia, Pavia, Italy, in 1979.

Since then, he has been working at the Department of Electronics of the University of Pavia in the field of electrooptics. His main research interests include injection modulation phenomena and chaos in lasers, electrical fiber sensors, the fiber gyroscope, active and passive fiber components for telecommunications and sensing, and transmission via diffused infrared radiation. In 1983, he became a Staff Researcher of the Department of Electronics of the University of Pavia and in 1992 he became an Associate Professor in the same institution. He is the author of more than 60 papers and holds three patents.

Dr. Annovazzi-Lodi is a member of AEI.

Alessandro Sciré was born in Rimini, Italy, in 1971. He graduated in electronics engineering from the University of Pavia, Pavia, Italy, in 1995 with a thesis on chaotic phenomena in lasers. He is currently working toward the Ph.D. degree in electronics engineering and computer science at the University of Pavia, working in the Optoelectronics group.

His main research interests are injection phoenomena in lasers and chaotic cryptography.

Marc Sorel was born in Sorengo, Switzerland, in 1971. He graduated from the University of Pavia, Pavia, Italy, in 1995, where he worked on semiconductor laser feedback and microoptic isolators.

He is presently still working in the Electrooptics group at the University of Pavia on speckle pattern phase reconstruction, with particular emphasis on interferometric applications, on chaos in laser sources, and on the electrooptic gyroscope.

Silvano Donati (M'75) graduated with a degree in physics from the University of Milan, Milan, Italy, in 1966.

For nine years he was with CISE (Milano), working on noise in photomultipliers and avalanche photodiodes, nuclear electronics and electrooptic instrumentation (laser telemetry, speckle pattern interferometry, gated vision in scattering media). In 1975, he joined the Department of Electronics, University of Pavia, Pavia, Italy, as internal lecturer and worked on feedback interferometers, fiber gyroscope, and noise in CCD's. In 1980, he became Full Professor of Optoelectronics, and since then his main research interests have been optical fiber sensors, passive fiber components for telecommunications, free-space and guided optical interconnections, and locking and chaos in lasers. He has authored or co-authored more than one hundred papers and holds four patents.

Dr. Donati is a member of AEI, APS, Optical Society of America, ISHM, and has actively served to organize several national and international meetings and schools in the steering and programme committees or as a chairman. He also worked in the standardization activity of CEI/IEC (CT-76 laser safety and CT-86 optical fibers).